The Canadian Journal of Mineralogy and Petrology
ISSN 2817-1713
Vol. 61, pp. 401-409 (2023)
DOI: 10.3749/2200064

MURPHYITE, $Pb(TeO)_4$, THE Te-ANALOGUE OF RASPITE, A NEW MINERAL FROM TOMBSTONE, ARIZONA, USA

HEXIONG YANG[§]

Department of Geosciences, University of Arizona, 1040 E. 4th Street, Tucson, Arizona 85721-0077, USA

XIANGPING GU

School of Geosciences and Info-Physics, Central South University, #932, South Lushan Road, Changsha, Hunan 410083, China

RONALD B. GIBBS AND ROBERT T. DOWNS

Department of Geosciences, University of Arizona, 1040 E. 4th Street, Tucson, Arizona 85721-0077, USA

ABSTRACT

A new mineral species, murphyite (IMA 2021-107), ideally $Pb(TeO_4)$, has been found from the Grand Central mine, Tombstone, Arizona, USA. It occurs as bladed or prismatic crystals on top of a quartz matrix. Associated minerals include chlorargyrite, emmonsite, ottoite, stolzite, scheelite, schieffelinite, quartz, and jarosite. Individual crystals of murphyite are up to $0.20 \times 0.05 \times 0.05$ mm in size. Twinning is common on {100}. Murphyite is colorless to very pale yellow in transmitted light, transparent with white streak and adamantine luster. It is brittle and has a Mohs hardness of ~3½, with perfect cleavage on {100}. The calculated density is 7.579 g/cm^3. Murphyite is insoluble in water or hydrochloric acid. An electron microprobe analysis yielded the empirical formula (based on 4 O *apfu*): $(Pb_{0.96}Fe_{0.03}Mn_{0.02})_{\Sigma 1.01}[(Te_{0.61}W_{0.38})_{\Sigma 0.99}O_4]$, which can be simplified to $Pb[(Te,W)O_4]$.

Murphyite is the Te-analogue of raspite, $Pb(WO_4)$, and represents the first mineral with Te^{6+} substituting for W^{6+} over 50%. It is monoclinic with space group $P2_1/a$ and unit-cell parameters $a = 13.6089(3)$, $b = 5.01750(10)$, $c = 5.5767(2)$ Å, $\beta = 107.9280(10)°$, $V = 362.302(17)$ Å^3, and $Z = 4$. Its crystal structure consists of distorted MO_6 (M = Te + W) octahedra sharing edges to form zigzag chains running parallel to [010]. These chains are linked together by PbO_7 polyhedra. Compared to raspite, the substitution of W^{6+} by Te^{6+}, which has a smaller ionic radius, results in a noticeable structural change: a significant decrease in MO_6 octahedral angle distortion, with a concomitant increase in both MO_6 octahedral volume and average Pb–O bond length. The unit-cell volume increases from 358.72(4) Å^3 for raspite to 362.302(17) Å^3 for murphyite. Raman spectroscopic data show that the major peak ascribable to M–O symmetrical stretching vibrations within the MO_6 octahedron is centered at 870 cm^{-1} for raspite but at 881 cm^{-1} for murphyite.

Keywords: murphyite, raspite, new mineral, crystal structure, X-ray diffraction, Raman spectra, Tombstone.

INTRODUCTION

The new mineral species, murphyite, ideally $Pb(TeO_4)$, was found at the Grand Central mine, Tombstone, Arizona, USA. It is named in honor of Mr. Bruce J. Murphy, who kindly provided a number of specimens for our research on Te-bearing minerals, including the specimen upon which the description of murphyite is based. Mr. Murphy received his B.S. degree in geological engineering from the University of Arizona and retired after a long career as an engineering geologist and consultant in the waste management industry. He has been a mineral collector for over 50 years, with a special interest in minerals from the Tombstone district, Arizona, USA, and has provided numerous samples for scientific research worldwide. The new mineral and its name have been approved by the Commission on New Minerals, Nomenclature and

[§] *Corresponding author e-mail address*: hyang@arizona.edu

Classification (CNMNC) of the International Mineralogical Association (IMA 2021-107). Co-type samples have been deposited in the Alfie Norville Gem and Mineral Museum (Catalogue # 22715) and the RRUFF Project (deposition # R210011) (http://rruff.info) at the University of Arizona.

Murphyite is the Te-analogue of raspite (Fujita *et al*. 1977), the monoclinic form of $Pb(WO_4)$, which is dimorphous with tetragonal $I4_1/a$ stolzite (Plakhov *et al*. 1970). Both raspite and stolzite are stable under ambient conditions, but relative to stolzite, raspite is rather rare in nature and transforms irreversibly to stolzite between 400 and 450 °C (Shaw & Claringbull 1955, Bastians *et al*. 2004). The compound $Pb(WO_4)$ possesses many unique physical properties, such as high density, short radiation length, short decay constant, and rather high radiation hardness (*e.g*., Arora & Chudasama 2007, George *et al*. 2008, Zheng *et al*. 2010, Yeom & Lim 2012). It has been used as a laser host material (Chen *et al*. 2001), a scintillator in high-energy physics detectors (Kobayashi *et al*. 1998, Hara *et al*. 1998, Annenkov *et al*. 2002), and an oxide ion conductor (Takai *et al*. 1999). Furthermore, considerable efforts have been devoted to synthesizing nanobelt or bamboo-leaf-like raspite to study its luminescence properties (George *et al*. 2008, Zheng *et al*. 2010, Yang & Huang 2012).

Raspite was originally described by Hlawatsch (1897) from Broken Hill, New South Wales, Australia. Shaw & Claringbull (1955) conducted the first X-ray structural analysis on raspite but were unable to locate the positions of the O atoms. Fujita *et al*. (1977) determined its crystal structure but with only isotropic displacement parameters for O atoms. A detailed structure refinement of raspite from the type locality, along with a Te-enriched raspite, $Pb(W_{0.56}Te_{0.44})O_4$, from Tombstone, Arizona, USA, was reported by Andrade *et al*. (2014). This current contribution describes the physical and chemical properties of murphyite, gives its crystal structure determined from single-crystal X-ray diffraction data, and discusses the structural variations between murphyite and raspite due to the $W^{6+} \leftrightarrow Te^{6+}$ substitution.

Sample Description and Experimental Methods

Occurrence, physical and chemical properties, and Raman spectra

Murphyite was found on a specimen (Fig. 1) collected from the Grand Central mine (31° 42′ 9″ N, 110° 3′ 43″ W), in the Tombstone district, Cochise County, Arizona, USA, about 1 km south of the town of Tombstone. The type specimen was originally collected by Sidney A. Williams and later obtained by Mr. Bruce J. Murphy. The Grand Central mine exploits

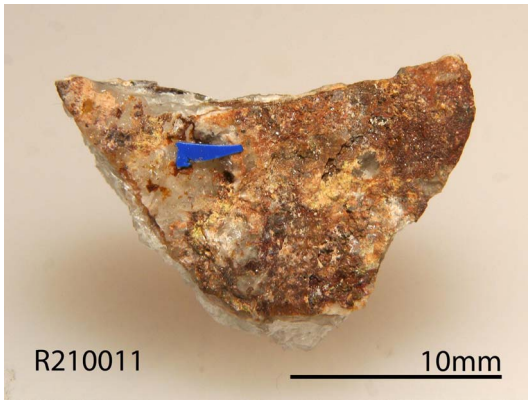

FIG. 1. A specimen on which the new mineral murphyite, indicated by the blue arrow, was found.

a Ag-Au-Pb-Cu-Zn deposit in which the ore, consisting principally of oxidized Ag- and Au-bearing galena, occurs in faulted and fractured portions of a large dike hosted by the Bisbee Group limestone. A good description of the history, geology, and mineralogy of the Tombstone district was provided by Williams (1980). Minerals associated with murphyite include chlorargyrite, emmonsite, ottoite, stolzite, scheelite, schieffelinite, quartz, and jarosite.

Murphyite occurs as bladed or prismatic crystals (Figs. 2, 3, and 4) on top of a quartz matrix. Individual crystals of murphyite are up to $0.20 \times 0.05 \times 0.05$ mm in size. Twinning is common on {100}, forming so-called fish-tail twins (Fig. 4). Murphyite is colorless to very pale yellow in transmitted light, transparent with white streak and adamantine luster. It is brittle and has a Mohs hardness of ~3½, with perfect cleavage on {100}. The density was not determined because it is greater than available density liquids and there is insufficient material for the direct measurement. The

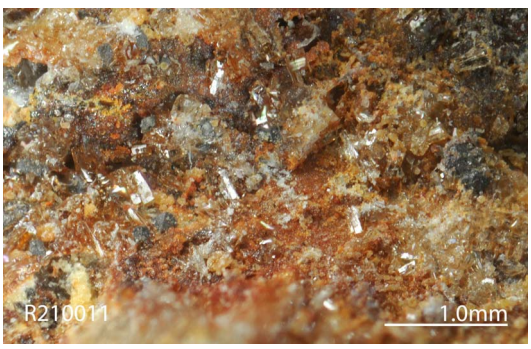

FIG. 2. A microscopic view of pale yellow prismatic or short bladed crystals murphyite on top of a quartz matrix.

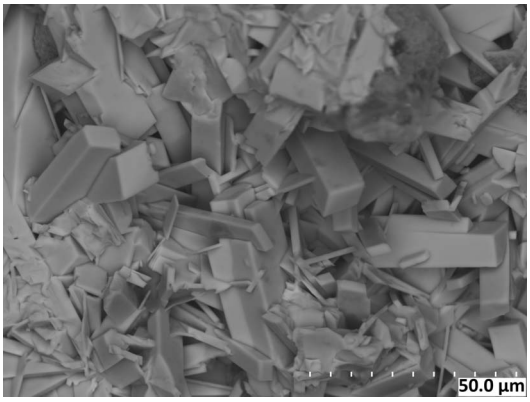

FIG. 3. A backscattered electron image of an aggregate of murphyite crystals.

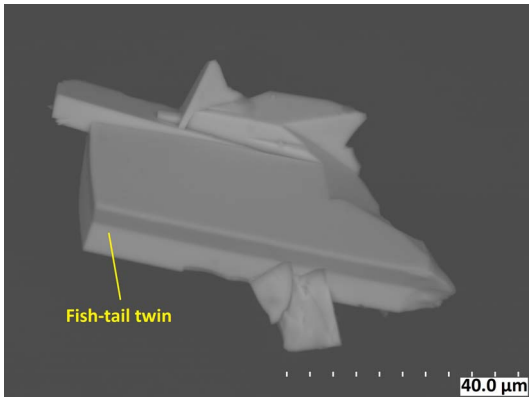

FIG. 4. A backscattered electron image of bladed murphyite crystals showing a fish-tail twin.

calculated density is 7.579 g/cm^3. No optical properties were measured because the indices of refraction are too high for measurement; no index liquids with $n > 2$ were available. The calculated average index of refraction is 2.15 for the empirical formula based on the Gladstone-Dale relationship (Mandarino 1981). Murphyite is insoluble in water or hydrochloric acid.

The chemical composition of murphyite was determined using a Cameca SX-100 electron microprobe (WDS mode, 20 kV, 20 nA, and a beam diameter of <1 µm). The standards used for the probe analysis are given in Table 1, along with the determined compositions (6 analysis points). The resultant chemical formula, calculated on the basis of 4 O *apfu*, is $(Pb_{0.96}Fe_{0.03}Mn_{0.02})_{\Sigma 1.01}[(Te_{0.61}W_{0.38})_{\Sigma 0.99}O_4]$, which can be simplified to $Pb[(Te,W)O_4]$.

The Raman spectrum of murphyite was collected on a randomly oriented crystal with a Thermo Almega microRaman system using a solid-state laser with a wavelength of 532 nm at the full power of 150 mW and a thermoelectric cooled CCD detector. The laser is partially polarized with 4 cm^{-1} resolution and a spot size of 1 µm.

X-ray crystallography

The X-ray powder diffraction data for murphyite (Table 2) were collected on a Rigaku Xtalab Synergy single-crystal diffractometer (Cu$K\alpha$ radiation) in Gandolfi powder mode at 50 kV and 1 mA. The unit-cell parameters refined using the program by Holland & Redfern (1997) are as follows: a = 13.584(2), b = 5.0354(8), c = 5.5681(7) Å, β = 107.973(8)°, and V = 362.26(2) Å^3.

Single-crystal X-ray diffraction data were collected from a $0.05 \times 0.04 \times 0.04$ mm fragment on a Bruker APEX2 CCD X-ray diffractometer equipped with graphite-monochromatized Mo$K\alpha$ radiation and with frame widths of 0.5° in ω and 30 s counting time per frame. The intensity data were corrected for X-ray absorption using the Bruker program SADABS. The systematic absences of reflections suggest the unique space group $P2_1/a$. The structure was solved and refined using SHELX2018 (Sheldrick 2015a, b). The refined ratio of Te *versus* W at the octahedral M (= Te + W) site is 0.60(1) Te + 0.40 W, very close to that (0.62 Te + 0.38 W) determined from the average of the electron microprobe analyses. The small amounts of Fe and Mn were assigned to the Pb site,

TABLE 1. CHEMICAL ANALYTICAL DATA (IN wt.%) FOR MURPHYITE

Constituent	Mean	Range	Stand. Dev.	Probe Standard
TeO_3	26.03	25.75–26.27	0.18	synthetic ZnTe
WO_3	21.46	21.09–21.87	0.24	scheelite
PbO	51.45	50.91–51.83	0.33	NBS_K0229
FeO	0.51	0.43–0.61	0.08	fayalite
MnO	0.34	0.24–0.42	0.06	rhodonite
Total	99.80	99.27–100.41	0.41	

TABLE 2. POWDER X-RAY DIFFRACTION DATA FOR MURPHYITE

I_{obs}%	d_{obs} (Å)	d_{cal} (Å)	h	k	l
0.6	6.548	6.461	2	0	0
2.3	5.325	5.296	0	0	1
3.2	4.913	4.905	2	0	$\bar{1}$
1.7	4.689	4.692	1	1	0
0.7	3.995	3.972	2	1	0
100.0	3.655	3.649	0	1	1
43.2	3.604	3.589	2	0	1
69.2	3.513	3.513	2	1	$\bar{1}$
34.4	3.235	3.230	4	0	0
27.8	2.926	2.923	2	1	1
51.4	2.768	2.768	2	0	$\bar{2}$
57.2	2.718	2.719	4	1	0
48.1	2.515	2.518	0	2	0
8.5	2.458	2.443	4	0	1
2.3	2.354	2.359	5	1	$\bar{1}$
12.9	2.223	2.240	2	2	$\bar{1}$
8.0	2.195	2.205	4	1	$\bar{2}$
6.6	2.129	2.131	3	2	$\bar{1}$
28.0	2.038	2.033	2	1	2
21.9	1.982	1.980	6	1	0
55.1	1.857	1.859	6	1	$\bar{2}$
8.2	1.812	1.810	6	0	1
22.6	1.744	1.740	2	1	$\bar{3}$
10.0	1.699	1.698	8	0	$\bar{1}$
6.7	1.670	1.679	6	2	$\bar{1}$
7.2	1.635	1.635	6	0	$\bar{3}$
7.3	1.592	1.606	1	3	$\bar{1}$
3.4	1.559	1.566	6	2	$\bar{2}$
6.5	1.539	1.538	8	1	0
3.6	1.519	1.510	2	1	3
12.6	1.487	1.493	2	2	$\bar{3}$
7.0	1.468	1.469	6	2	1
11.1	1.408	1.418	3	3	$\bar{2}$
3.8	1.385	1.380	4	0	3
3.6	1.338	1.346	6	3	$\bar{1}$
4.7	1.286	1.289	9	1	$\bar{3}$
4.8	1.243	1.241	8	2	1
5.0	1.213	1.210	4	2	3

with Mn treated as Fe, as the X-ray structure analysis is insufficient to distinguish them due to their similar X-ray scattering powers. All atoms were refined anisotropically. Refinement statistics are given in Table 3. Final atomic coordinates and displacement parameters are given in Tables 4 and 5, respectively. Selected bond distances are presented in Table 6[1]. The bond-valence sums were calculated using the parameters given by Brese and O'Keeffe (1991) (Table 7). The final chemical formula calculated from the structure refinement is $(Pb_{0.95}\,Fe_{0.05})_{\Sigma 1}[(Te_{0.60}W_{0.40})_{\Sigma 1}O_4]$.

[1] Supplementary Data are available from the Depository of Unpublished Data on the MAC website (http://mineralogicalassociation.ca/), document "Murphyite, CM61, 22-00064".

Results and Discussion

Crystal structure

Murphyite is the Te-analogue of raspite, $Pb(WO_4)$ (Fujita *et al*. 1977, Andrade *et al*. 2014). Its crystal structure consists of distorted MO_6 octahedra sharing edges to form zigzag chains running parallel to [010]. These octahedral chains are linked together by seven-coordinated Pb^{2+} cations (Fig. 5). Compared to raspite, $Pb(WO_4)$, the partial substitution of the smaller Te^{6+} ($r = 0.56$ Å) for larger W^{6+} ($r = 0.60$ Å) (Shannon 1976) results in a noticeable structural change: a significant decrease in the MO_6 octahedral angle distortion, measured by the octahedral angle variance (Robinson *et al*. 1971), from 104 to 84, with a concomitant increase in the MO_6 octahedral volume and the average Pb–O bond length (Table 6). As a consequence, the unit-cell volume (V) increases from 358.72(4) Å^3 for raspite to 362.302(17) Å^3 for murphyite (Table 3). The greater distortion of the MO_6 octahedron in raspite stems primarily from the so-called second-order Jahn-Teller (SOJT) effect of W^{6+}, owing to its empty d-shell (*e.g*., Ra *et al*. 2003, Lufaso & Woodward 2004). In contrast, Te^{6+} has a full d-shell, which suppresses part of the SOJT distortions. In other words, two competing factors take place with the substitution of Te^{6+} for W^{6+}: (1) the replacement of W^{6+} by Te^{6+} should lead to decreased V because the ionic radius of Te^{6+} is smaller, and (2) increased Te^{6+} in the site will reduce the MO_6 octahedral distortion, which lessens the packing efficiency of the structure (Andrade *et al*. 2014), thus increasing V. As shown in Table 3, V increases from 358.72(4) Å^3 for raspite (Te = 0) to 363.19(15) Å^3 for Te-enriched raspite (Te = 44%) (Andrade *et al*. 2014), indicating that the second factor dominates over the first. However, V is reduced from 363.19(15) Å^3 for Te-enriched raspite to 362.302(17) Å^3 for murphyite (Te = 60%), indicating that the further addition of Te^{6+} actually reverses the net effect of the two competing factors. Based on this observation, an even smaller V for pure murphyite ($PbTeO_4$) may be expected, pointing to a non-ideal solid solution between $Pb(WO_4)$ and $Pb(TeO_4)$. Nevertheless, due to the limited data, it is unclear whether the decrease in V occurs at Te $<44\%$ or $>44\%$.

TABLE 3. COMPARISON OF CRYSTALLOGRAPHIC DATA FOR RASPITE AND MURPHYITE

	Raspite	Te-enriched raspite	Murphyite
Ideal formula	$PbWO_4$	$PbWO_4$	$PbTeO_4$
Empirical formula	$PbWO_4$	$Pb(W_{0.54}Te_{0.46})O_4$	$Pb(Te_{0.62}W_{0.38})O_4$
Crystal symmetry	Monoclinic	Monoclinic	Monoclinic
Space group	$P2_1/a$	$P2_1/a$	$P2_1/a$
a (Å)	13.5773(8)	13.621(3)	13.6089(3)
b (Å)	4.9806(3)	5.0187(12)	5.01750(10)
c (Å)	5.5670(3)	5.5858(14)	5.5767(2)
β (°)	107.658(3)	107.979(5)	107.9280(10)
V (Å^3)	358.72(4)	363.19(15)	362.302(17)
Z	4	4	4
ρ_{cal} (g/cm^3)	8.43	7.87	7.58
2θ range for data collection (°)	≤65.15	≤65.34	≤65.32
No. of reflections collected	8180	5113	5224
No. of independent reflections	1315	1336	1330
No. of reflections with $I > 2\sigma(I)$	1156	1211	1138
No. of parameters refined	56	57	58
R(int)	0.048	0.033	0.035
Final R_1 factor [$I > 2\sigma(I)$]	0.025	0.026	0.029
Final wR_2 factor [$I > 2\sigma(I)$]	0.053	0.052	0.047
Goodness-of-fit	1.06	1.13	1.06
Reference	Andrade *et al.* (2014)	Andrade *et al.* (2014)	This study

TABLE 4. FRACTIONAL ATOMIC COORDINATES AND EQUIVALENT ISOTROPIC DISPLACEMENT PARAMETERS (Å^2) FOR MURPHYITE

Atom	x	y	z	U_{eq}
Pb	0.15764 (2)	0.19928 (6)	0.16006 (6)	0.02149 (11)
M	0.07390 (2)	0.75045 (6)	0.59889 (6)	0.00968 (12)
O1	0.0200 (3)	0.0557 (9)	0.7269 (8)	0.0148 (10)
O2	0.0611 (3)	0.4358 (8)	0.3918 (9)	0.0137 (10)
O3	0.1472 (4)	0.6299 (10)	0.9065 (9)	0.0211 (12)
O4	0.1856 (3)	0.8857 (9)	0.5272 (9)	0.0192 (11)

Note: The refined occupancies for Pb and *M* are [0.952(10) Pb + 0.048(10) Fe] and [0.598(17) Te + 0.402(17) W], respectively.

TABLE 5. ATOMIC DISPLACEMENT PARAMETERS (Å^2) FOR MURPHYITE

Atom	U^{11}	U^{22}	U^{33}	U^{12}	U^{13}	U^{23}
Pb	0.01819 (16)	0.02458 (17)	0.02284 (17)	−0.00095 (11)	0.00800 (11)	−0.00700 (11)
M	0.01000 (18)	0.00708 (16)	0.01115 (17)	−0.00003 (11)	0.00207 (11)	0.00120 (11)
O1	0.016 (2)	0.014 (2)	0.013 (2)	0.0011 (17)	0.0019 (18)	−0.0004 (17)
O2	0.014 (2)	0.010 (2)	0.022 (3)	−0.0058 (17)	0.013 (2)	−0.0011 (18)
O3	0.021 (3)	0.023 (3)	0.015 (2)	−0.004 (2)	0.000 (2)	0.008 (2)
O4	0.012 (2)	0.021 (2)	0.023 (3)	−0.0014 (19)	0.003 (2)	0.006 (2)

TABLE 6. SELECTED BOND DISTANCES (Å) FOR RASPITE AND MURPHYITE

	Raspite	Te-enriched raspite	Murphyite
	$Pb(WO_4)$	$Pb(W_{0.56}Te_{0.44})O_4$	$Pb(Te_{0.60}W_{0.40})O_4$
M–O1	1.886(5)	1.929(5)	1.928(4)
M–O1′	2.192(5)	2.118(5)	2.109(4)
M–O2	1.930(5)	1.941(5)	1.932(4)
M–O2′	2.116(5)	2.080(5)	2.076(4)
M–O3	1.767(6)	1.800(5)	1.802(5)
M–O4	1.800(5)	1.807(5)	1.818(4)
<*M*–O>	1.945	1.946	1.944
OV	9.426	9.472	9.454
OQE	1.038	1.029	1.028
OAV	104.1	85.4	83.77
Pb–O1	2.663(5)	2.665(5)	2.661(4)
Pb–O1′	2.773(6)	2.958(5)	2.969(4)
Pb–O2	2.323(5)	2.412(4)	2.419(4)
Pb–O3	2.545(6)	2.571(5)	2.562(5)
Pb–O3′	2.946(6)	2.823(6)	2.815(5)
Pb–O4	2.486(5)	2.495(5)	2.485(5)
Pb–O4′	2.529(6)	2.519(5)	2.517(5)
<Pb–O>	2.610	2.635	2.632
Polyhedral volume	23.923	24.295	24.242
Reference	Andrade *et al.* (2014)	Andrade *et al.* (2014)	This study

Note: *M* = (Te + W); OV = octahedral volume, OQE = octahedral quadratic elongation, OAV = octahedral angle variance (Robinson *et al.* 1971).

Raman spectra

Raspite has been previously investigated with Raman spectroscopy (Bastians *et al*. 2004, Yang & Huang 2012, Andrade *et al*. 2014) and detailed assignments of its major Raman bands have been proposed by Bastians *et al*. (2004). Figure 6 shows the Raman spectra for murphyite, Te-enriched raspite [$Pb(W_{0.56}Te_{0.44})O_4$], and raspite (Andrade *et al*. 2014). The spectra of the three minerals are similar, but some differences among them are also discernible. Specifically, due to the partial Te^{6+} substitution for W^{6+} (Te–W disordering) in murphyite and Te-enriched raspite, most Raman bands for these two minerals are considerably broader than the corresponding ones for raspite. Most remarkably, between 840 and 920 cm^{-1} there is only one strong, sharp band at 870 cm^{-1} for raspite, which is ascribable to the W–O symmetrical stretching vibrations within the WO_6 octahedron (Bastians *et al*. 2004, Frost *et al*. 2004, Yang & Huang 2012). In contrast, there are two strong overlapped bands in the same region for Te-enriched raspite, the major one at 881 cm^{-1} and a shoulder at 871 cm^{-1} (Fig. 6), which may be assigned to Te–O and W–O symmetrical stretching vibrations within the MO_6 octahedron (M = Te, W), respectively, as the Te–O bond is shorter and stronger with greater covalent nature than the W–O bond (Wang *et al*. 2010). Interestingly, as with raspite, murphyite also displays only one strong, sharp band between 840 and 920 cm^{-1}, not two overlapping bands, as observed for Te-enriched raspite, despite the fact that it has 38% W^{6+} substituting for Te^{6+}. Nevertheless, the position of this major band is shifted to 881 cm^{-1}, indicating the dominant presence of Te^{6+} at the *M* site in murphyite.

As six-coordinated W^{6+}, Mo^{6+}, and Te^{6+} have similar ionic radii, which are 0.60, 0.59, and 0.56 Å (Shannon 1976), respectively, extensive solid solutions

TABLE 7. BOND-VALENCE SUMS FOR MURPHYITE

	Pb	*M*	Sum
O1	0.227	0.971	1.891
	0.099	0.595	
O2	0.437	0.961	2.049
		0.651	
O3	0.296	1.363	1.809
	0.150		
O4	0.365	1.307	2.007
	0.335		
Sum	1.908	5.847	

Note: The bond valence sum for *M* was calculated based on (0.60 Te^{6+} + 0.40 W^{6+}).

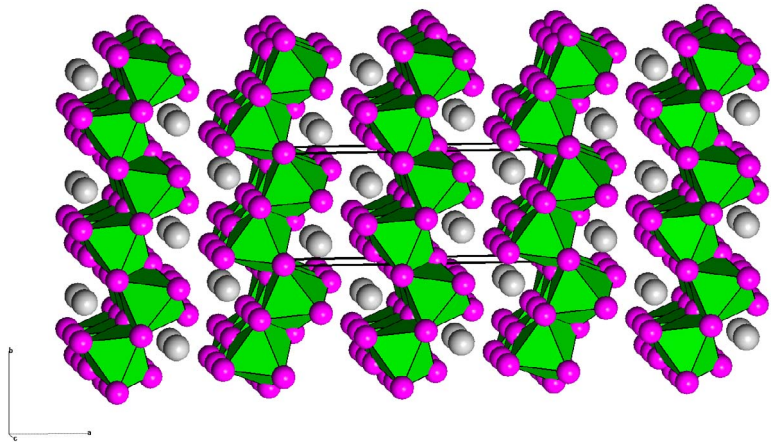

FIG. 5. The crystal structure of murphyite. The octahedra, large gray spheres, and small purple spheres represent the MO_6 (M = Te + W) groups, Pb atoms, and O atoms, respectively.

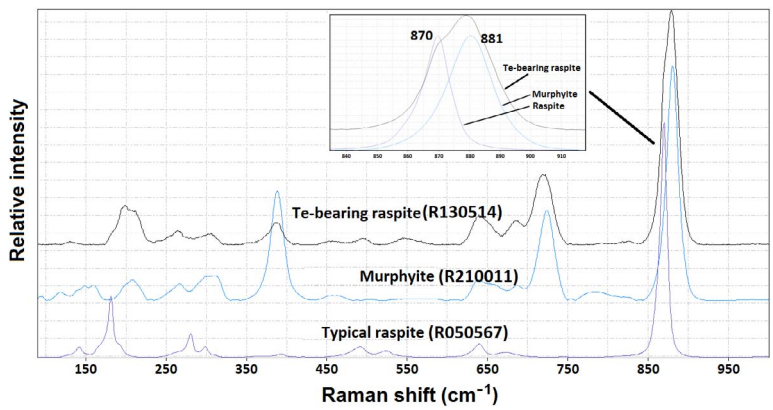

FIG. 6. The Raman spectra of murphyite, raspite, and Te-enriched raspite.

among them can be expected. This is indeed the case for synthetic compounds, such as $LaNi_{0.8}M_{0.2}O_3$ (M = Mo^{6+}, Te^{6+}, W^{6+}) (Alvarez *et al*. 1995, 1997), $Pb_2Mg(W_{1-x}Te_x)O_6$ (Rivezzi & Sciau 1998), $LiY(W_{1-x}Te_x)O_8$ (Wang *et al*. 2010), $KNaMO_2F_4$ (M = Mo^{6+}, W^{6+}) (Pinlac *et al*. 2011), $Bi_2(W_{1-x}Te_x)O_6$ (Waehayee *et al*. 2021), and a variety of Mo-Te mixed oxides used as catalysts in the gas phase selective oxidation of hydrocarbons (*e.g*., Botella *et al*. 2002, 2009, López Nieto *et al*. 2003, Holmberg *et al*. 2007). However, there has been no report thus far for the significant substitution of Te^{6+} for W^{6+} or Mo^{6+} in minerals, despite the common substitution between W^{6+} and Mo^{6+}, as in the scheelite group of minerals. Therefore, murphyite represents the first natural example with Te^{6+} substituting for W^{6+} over 50%.

ACKNOWLEDGMENTS

We are grateful for the constructive comments by Dr. Anthony Kampf and Dr. Andrew McDonald. This study was funded by the Feinglos family and Mr. Michael M. Scott.

REFERENCES

ALVAREZ, I., VEIGA, M.I., & PICO, C. (1995) Synthesis and structural characterization of a new perovskite series derived from $LaNiO_3$: $La_5Ni_4MO_{15}$ (M = Mo, Te, W). *Journal of Materials Chemistry* **5**, 1049–1051.

ALVAREZ, I., VEIGA, M.I., & PICO, C. (1997) Structural characterization and electronic properties of A-substituted $LaNi_{0.8}M_{0.2}O_3$ (A = Ca, Sr; M = Te, W) perovskites. *Solid State Ionics* **93**, 329–334.

ANDRADE, M.B., YANG, H., DOWNS, R.T., JENKINS, R.A., & FAY, I. (2014) Te-rich raspite, $Pb(W_{0.56}Te_{0.44})O_4$, from Tombstone, Arizona, U.S.A.: The first natural example of Te^{6+} substitution for W^{6+}. *American Mineralogist* **99**, 1507–1510.

ANNENKOV, A.A., KORZHIK, M.V., & LECOQ, P. (2002) Lead tungstate scintillation material. *Nuclear Instruments and Methods in Physics Research* **A490**, 30–50.

ARORA, S.K. & CHUDASAMA, B. (2007) Flux growth and optoelectronic study of $PbWO_4$ single crystals. *Crystal Growth & Design* **7**, 296–299.

BASTIANS, S., CRUMP, G., GRIFFITH, W.P., & WITHNALL, R. (2004) Raspite and studtite: Raman spectra of two unique minerals. *Journal of Raman Spectroscopy* **35**, 726–731.

BOTELLA, P., LÓPEZ NIETO, J.M., & SOLSONA, B. (2002) Selective oxidation of propene to acrolein on Mo-Te mixed oxides catalysts prepared from ammonium telluromolybdates. *Journal of Molecular Catalysis A: Chemical* **184**, 335–347.

BOTELLA, P., GARCÍA-GONZÁLEZ, E., SOLSONA, B., RODRÍGUEZ-CASTELLÓN, E., GONZÁLEZ-CALBET, J.M., & LÓPEZ NIETO, J.M. (2009) Mo-containing tetragonal tungsten bronzes. The influence of tellurium on catalytic behaviour in selective oxidation of propene. *Journal of Catalysis* **265**, 43–53.

BRESE, N.E. & O'KEEFFE, M. (1991) Bond-valence parameters for solids. *Acta Crystallographica* **B47**, 192–197.

CHEN, W., INAGAWA, Y., OMATSU, T., TATEDA, M., TAKEUCHI, N., & USUKI, Y. (2001) Diode-pumped, self-stimulating, passively Q-switched Nd^{3+}: $PbWO_4$ Raman laser. *Optical Communications* **94**, 401–407.

FROST, R.L., DUONG, L., & WEIER, M. (2004) Raman microscopy of selected tungstate minerals. *Spectrochimica Acta* **A60**, 1853–1859.

FUJITA, T., KAWADA, I., & KATO, K. (1977) Raspite from Broken Hill. *Acta Crystallographica* **B33**, 162–164.

GEORGE, T., JOSEPH, S., SUNNY, A.T., & MATHEW, S. (2008) Fascinating morphologies of lead tungstate nanostructures by chimie douce approach. *Journal of Nanoparticle Research* **10**, 567–575.

HARA, K., ISHII, M., NIKL, M., TAKANO, H., TANAKA, M., TANJI, K., & USUKI, Y. (1998) La-doped $PbWO_4$, scintillating crystals grown in large ingots. *Nuclear Instruments and Methods in Physics Research* **A414**, 325–331.

HLAWATSCH, C. (1897) Ueber Stolzit und Raspit von Brokenhill. *Zeitschrift für Krystallographie und Mineralogie* **29**, 130–139.

HOLLAND, T.J.B. & REDFERN, S.A.T. (1997) Unit cell refinement from powder diffraction data: The use of regression diagnostics. *Mineralogical Magazine*, **61**, 65–77.

HOLMBERG, J., WAGNER, J.B., HAGGBLAD, R., HANSEN, S., WALLENBERG, L.R., & ANDERSSON, A. (2007) Catalytic and structural effects of W-substitution in M2 Mo-V-Te-oxide for propene ammoxidation. *Catalysis Today* 85, 153–160.

KOBAYASHI, M., ISHII, M., & USUKI, Y. (1998) Comparison of radiation damage in different $PbWO_4$ scintillating crystals. *Nuclear Instruments and Methods in Physics Research* **A406**, 442–450.

LÓPEZ NIETO, J.M., BOTELLA, P., SOLSONA, B., & OLIVER, J.M. (2003) The selective oxidation of propane on Mo-V-Te-Nb-O catalysts: The influence of Te-precursor. *Catalysis Today* **81**, 87–94.

LUFASO, M.W. & WOODWARD, P.M. (2004) Jahn-Teller distortions, cation ordering and octahedral tilting in perovskites. *Acta Crystallographica* **B60**, 10–20.

MANDARINO, J.A. (1981) The Gladstone-Dale relationship. IV. The compatibility concept and its application. *The Canadian Mineralogist* **19**, 441–450.

PINLAC, R.A.F., STERN, C.L., & POEPPELMEIER, K.R. (2011) New layered oxide-fluoride perovskite: $KNaNbOF_5$ and $KNaMO_2F_4$ ($M = Mo^{6+}$, W^{6+}). *Crystals* **1**, 3–14.

PLAKHOV, G.F., POBEDIMSKAYA, E.A., SIMONOV, M.A., & BELOV, N.V. (1970) The crystal structure of $PbWO_4$. *Kristallografiya* **15**, 1067–1068.

RA, H.-S., OK, K.M., & HALASYAMANI, P.S. (2003) Combining second-order Jahn-Teller distorted cations to create highly efficient SHG materials: Synthesis, characterization, and NLO properties of BaTeMO (M = Mo or W). *Journal of the American Chemical Society* **125**, 7764–7765.

RIVEZZI, N. & SCIAU, P. (1998) Etude de la solution solide entre tungstate et tellurate de magnesium: $Pb_2MgW_xTe_{(1-x)}O_6$. *Journal of Solid State Chemistry* **139**, 332–341.

ROBINSON, K., GIBBS, G.V., & RIBBE, P.H. (1971) Quadratic elongation: A quantitative measure of distortion in coordination polyhedra. *Science* **172**, 567–570.

SHANNON, R.D. (1976) Revised effective ionic radii and systematic studies of interatomic distances in halides and chalcogenides. *Acta Crystallographica* **A32**, 751–767.

SHAW, R. & CLARINGBULL, G.F. (1955) X-ray study of raspite (monoclinic $PbWO_4$). *American Mineralogist* **40**, 933.

SHELDRICK, G.M. (2015a) SHELXT – Integrated space-group and crystal structure determination. *Acta Crystallographica* **A71**, 3–8.

SHELDRICK, G.M. (2015b) Crystal structure refinement with SHELX. *Acta Crystallographica* **C71**, 3–8.

TAKAI, S., SUGIURA, K., & ESAKA, T. (1999) Ionic conduction properties of $Pb_{1-x}M_xWO_{4+\delta}$ (M = Pr, Tb). *Materials Research Bulletin* **34**, 193–202.

WAEHAYEE, A., PONGSAWAKUL, C., NGOIPALA, A., PHONSUKSAWANG, P., JIAMPRASERTBOON, A., WANNAPAIBOON, S., NAKAJIMA, H., BUTBUREE, T., SUTHIRAKUN, S., &

SIRITANON, T. (2021) Promoting superoxide generation in Bi_2WO_6 by less electronegative substitution for enhanced photocatalytic performance: An example of Te doping. *Catalysis Science & Technology* **11**, 6291–6304.

WANG, L., BIAN, J.J., & GUO, G.H. (2010) Phase transition and microwave dielectric properties of $LiY(W_{1-x}Te_x)_2O_8$ ($0.0 \leq x \leq 0.2$). *Materials Chemistry and Physics* **124**, 748–750.

WILLIAMS, S.A. (1980) The Tombstone district, Cochise County, Arizona. *Mineralogical Record* **11**, 251–256.

YANG, X. & HUANG, J. (2012) Phase transformation of lead tungstate at normal temperature from tetragonal structure to monoclinic structure. *Journal of the American Ceramic Society* **95**, 3334–3338.

YEOM, T.H. & LIM, A.R. (2012) Magnetic resonance studies on ^{207}Pb nuclei and paramagnetic impurities in $PbWO_4$:Eu, $PbWO_4$:Gd, and pure $PbWO_4$ single crystals. *Journal of Molecular Structure* **1027**, 44–48.

ZHENG, C., HU, C., CHEN, X., XIONG, Y., XU, J., WAN, B., & HUANG, L. (2010) Raspite $PbWO_4$ nanobelts: Synthesis and properties. *CrystEngComm* **12**, 3277–3282.

Received October 20, 2022. Revised manuscript accepted January 11, 2023.

This manuscript was handled by Associate Editor James Evans and Editor Andrew McDonald.